OPTIMIZING DDPM SAMPLING WITH SHORTCUT FINE-TUNING

Ying FanUniversity of Wisconsin-Madison
yfan87@wisc.edu

Kangwook Lee University of Wisconsin-Madison kangwook.lee@wisc.edu

ABSTRACT

In this study, we propose *Shortcut Fine-Tuning (SFT)*, a new approach for addressing the challenge of fast sampling of pretrained Denoising Diffusion Probabilistic Models (DDPMs). SFT advocates for the fine-tuning of DDPM samplers through the direct minimization of Integral Probability Metrics (IPM), instead of learning the backward diffusion process. This enables samplers to discover an alternative and more efficient sampling shortcut, deviating from the backward diffusion process. We also propose a new algorithm that is similar to the policy gradient method for fine-tuning DDPMs by proving that under certain assumptions, the gradient descent of diffusion models is equivalent to the policy gradient approach. Through empirical evaluation, we demonstrate that our fine-tuning method can further enhance existing fast DDPM samplers, resulting in sample quality comparable to or even surpassing that of the full-step model across various datasets.

1 Introduction

Denoising diffusion probabilistic models (DDPMs) [Ho et al., 2020] are parameterized stochastic Markov chains, which are learned by gradually adding Gaussian noises to the data as the forward process, computing the backward process via posterior, and then training the DDPM sampler to match the backward process. Advances in DDPM [Nichol and Dhariwal, 2021, Dhariwal and Nichol, 2021] have shown its potential to rival GANs [Goodfellow et al., 2014] in generative tasks. One drawback of DDPM is that a large number of steps T is needed. As a result, there is a line of work dedicated to sampling fewer $T' \ll T$ steps to achieve better performance. Most works are dedicated to better approximating the backward process as stochastic differential equations (SDEs) with fewer steps, generally via better noise estimation and sub-sequence scheduling: [Kong and Ping, 2021, San-Roman et al., 2021, Lam et al., 2021, Watson et al., 2021a, Jolicoeur-Martineau et al., 2021, Bao et al., 2021, 2022]. Other works aim at approximating the backward process by fewer steps via changing the noise distribution to non-gaussian [Nachmani et al., 2021, Xiao et al., 2021].

To our best knowledge, existing fast samplers of DDPM stick to imitating the backward process. If we view data generation as a Reinforcement Learning (RL) task and the backward process as a demonstration to generate data from noise, imitating the backward process could be viewed as imitation learning [Hussein et al., 2017], which is one way to learn a generative model as policy. Naturally, one may wonder if we can do better than pure imitation, since learning via imitation is generally useful but rarely optimal. It generally takes extra interactions with the "environment" to find an optimal one [Vecerik et al., 2017].

Motivated by the above observation, we study the following underexplored question:

Can we improve DDPM sampling by **not** following the backward process?

In this work, we show that this is indeed possible. We fine-tune pretrained DDPM samplers by directly minimizing an integral probability metric (IPM) and show that finetuned DDPM samplers have significantly better generation qualities. In this way, we can still enjoy diffusion models' multistep capabilities with no need to change the noise distribution, and improve the performance with fewer steps.

More concretely, we first show that performing gradient descent of the DDPM sampler w.r.t. the IPM is equivalent to policy gradient, which echoes the aforementioned RL view but with a changing reward from the optimal critic function

¹There is another line of work dedicated to fast sampling DDIM [Song et al., 2020a] that uses deterministic Markov chains, which we will discuss in Section 5.

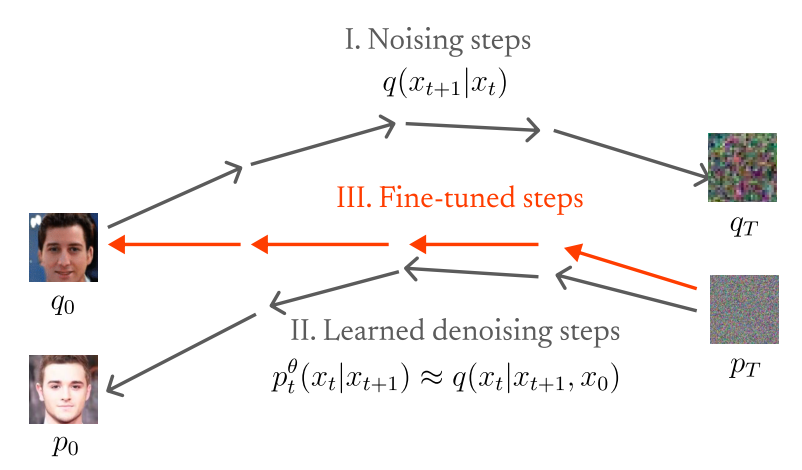


Figure 1: A visual illustration of the key idea of Shortcut Fine-Tuning (SFT). DDPMs aim at learning the backward diffusion model, but this approach is limited with a small number of steps. We propose the idea of *not* following the backward process and exploring other unexplored paths that can lead to improved data generation. To this end, we directly minimize an IPM and develop a policy gradient-like optimization algorithm. Our experimental results show that one can significantly improve data generation quality by fine-tuning a pretrained DDPM model with SFT.

in IPM. In addition, we provide a surrogate function that can give insights for monotonic improvements. Finally, we provide a fine-tuning algorithm with alternative updates between the critic and the generator.

We summarize our main contributions as follows:

- (Section 4.1) We propose a novel algorithm to fine-tune DDPM samplers with direct IPM minimization, and we show that performing gradient descent of diffusion models w.r.t. IPM is equivalent to policy gradient.
- (Section 4.2) We present a surrogate function of IPM in theory, which provides insights on conditions for monotonic improvement and algorithm design.
- (Section 4.3.2) We propose a regularization for the critic based on the baseline function, which shows benefits for the policy gradient training.
- (Section 6) Empirically, we show that our fine-tuning can improve DDPM sampling performance in two cases: when T itself is small, and when T is large but using a fast sampler where $T' \ll T$. In both cases, our fine-tuning achieves comparable or even higher sample quality than the DDPM with 1000 steps using 10 sampling steps.

2 Background

2.1 Denoising Diffusion Probabilistic Models (DDPM)

Here we consider denoising probabilistic diffusion models (DDPM) introduced in Ho et al. [2020]. Consider data distribution $x_0 \sim q_0, x_0 \in \mathbb{R}^n$. Define the forward noising process: for $t \in [0, ..., T-1]$,

$$q(x_{t+1}|x_t) := \mathcal{N}(\sqrt{1 - \beta_t}x_t, \beta_t I), \tag{1}$$

where $x_1,...,x_T$ are variables of the same dimensionality as $x_0, \beta_{1:T}$ is the variance schedule.

We can compute the posterior as a backward process:

$$q(x_t|x_{t+1},x_0) = \mathcal{N}(\tilde{\mu}_{t+1}(x_{t+1},x_0),\tilde{\beta}_{t+1}I),$$
where $\tilde{\mu}_{t+1}(x_{t+1},x_0) = \frac{\sqrt{\bar{\alpha}_t}\beta_t}{1-\bar{\alpha}_{t+1}}x_0 + \frac{\sqrt{\alpha_{t+1}}(1-\bar{\alpha}_t)}{1-\bar{\alpha}_{t+1}}x_{t+1}, \alpha_{t+1} = 1 - \beta_{t+1}, \bar{\alpha}_{t+1} = \prod_{s=1}^{t+1}\alpha_s.$
(2)

We define a DDPM sampler parameterized by θ , which generates data starting from some pure noise $x_T \sim p_T$:

$$x_{T} \sim p_{T} = \mathcal{N}(0, I),$$

$$x_{t} \sim p_{t}^{\theta}(x_{t}|x_{t+1}),$$

$$p_{t}^{\theta}(x_{t}|x_{t+1}) := \mathcal{N}(\mu_{t+1}^{\theta}(x_{t+1}), \Sigma_{t+1}),$$
(3)

where Σ_{t+1} is generally chosen as $\beta_{t+1}I$ or $\tilde{\beta}_{t+1}I$. ²

Define

$$p_{x_{0:T}}^{\theta} := p_T(x_T) \prod_{t=0}^{T-1} p_t^{\theta}(x_t | x_{t+1}), \tag{4}$$

and we have $p_0^{\theta}(x_0) = \int p_{x_{0:T}}^{\theta}(x_{0:T}) dx_{1:T}$.

The sampler is trained via minimizing the ELBO:

$$\mathbb{E}_{q_0} \left[-\log p_0^{\theta}(x_0) \right] \leqslant \mathbb{E}_q \left[-\log \frac{q(x_{1:T}|x_0)}{p_{x_{0:T}}^{\theta}(x_{0:T})} \right], \tag{5}$$

which is equivalent to minimizing the sum of KL divergence below:

$$J = \sum_{t=0}^{T-1} D_{KL}(q(x_t|x_{t+1}, x_0), p_t^{\theta}(x_t|x_{t+1})).$$
(6)

Optimizing the above loss can be viewed as matching the conditional generator $p_t^{\theta}(x_t|x_{t+1})$ with the posterior distribution $q(x_t|x_{t+1},x_0)$ for each step. Song et al. [2020b] have also shown that J is equivalent to score-matching loss when formulating the forward and backward process as a discrete version of stochastic differential equations.

2.2 Integral Probability Metrics (IPM)

Given \mathcal{A} as a set of parameters s.t. for each $\alpha \in \mathcal{A}$, it defines a critic $f_{\alpha} : \mathbb{R}^n \to \mathbb{R}$. Given a critic f_{α} and two distributions p_0^{θ} and q_0 , we define

$$g(p_0^{\theta}, f_{\alpha}, q_0) := \underset{x_0 \sim p_0^{\theta}}{\mathbb{E}} [f_{\alpha}(x_0)] - \underset{x_0 \sim q_0}{\mathbb{E}} [f_{\alpha}(x_0)]. \tag{7}$$

Let

$$\Phi(p_0^{\theta}, q_0) := \sup_{\alpha \in A} g(p_0^{\theta}, f_{\alpha}, q_0). \tag{8}$$

If \mathcal{A} satisfies that $\forall \alpha \in \mathcal{A}$, $\exists \alpha' \in \mathcal{A}$, s.t. $f_{\alpha'} = -f_{\alpha}$, then $\Phi(p_{\theta}, q)$ is a pseudo metric over the probability space of \mathbb{R}^n , making it so-called integral probability metrics (IPM).

In this paper, we consider \mathcal{A} that makes $\Phi(p_0^\theta,q_0)$ an IPM. For example, when $\mathcal{A}=\{\alpha:||f_\alpha||_L\leqslant 1\}, \Phi(p_0^\theta,q_0)$ is the Wasserstein-1 distance; when $\mathcal{A}=\{\alpha:||f_\alpha||_\infty\leqslant 1\}, \Phi(p_0^\theta,q_0)$ is the total variation distance; it also includes maximum mean discrepancy (MMD) when \mathcal{A} defines all functions in Reproducing Kernel Hilbert Space (RKHS).

3 Motivation

3.1 Issues with Existing DDPM Samplers

Here we review the existing issues with DDPM samplers 1) when T is not large enough, and 2) when the number of sampling steps $T' \ll T$, which inspires us to design our fine-tuning algorithm.

Case 1. Issues caused by training DDPM with a small T (Fig 1). Given a score-matching loss J, the upper bound on Wasserstein-2 distance is given by Kwon et al. [2022]:

$$W_2(p_0^{\theta}, q_0) \le \mathcal{O}(\sqrt{J}) + I(T)W_2(p_T, q_T),$$
(9)

where I(T) is non-exploding and $W_2(p_T,q_T)$ decays exponentially with T when $T\to\infty$. From the inequality above, one sufficient condition for the score-matching loss J to be viewed as optimizing the Wasserstein distance is when T is large enough such that $I(T)W_2(p_T,q_T)\to 0$. Now we consider the case when T is small and $p_T\not\approx q_T$. The upper bound in Eq. (9) can be high since $W_2(p_T,q_T)$ is not neglectable. As shown in Fig 1, pure imitation $p_t^\theta(x_t|x_{t+1})\approx q(x_t|x_{t+1},x_0)$ would not lead the model exactly to q_0 when p_T and q_T are not close enough.

²In this work we consider a DDPM sampler with a fixed variance schedule $\beta_{1:T}$, while it could also be learned as in Nichol and Dhariwal [2021].

³Recall that we need small Gaussian noises for the DDPM sampler to work [Ho et al., 2020], so a small T means q_T is not very noised, and $p_T \not\approx q_T$.

Case 2. Issues caused by a smaller number of sub-sampling steps (T') (Fig 6 in Appendix A). We consider DDPM sub-sampling and other fast sampling techniques, where T is large enough s.t. $p_T \approx q_T$, but we try to sample with fewer sampling steps (T'). It is generally done by choosing τ to be an increasing sub-sequence of T' steps in [0,T] starting from 0. Many works have been dedicated to finding a subsequence and variance schedule to make the sub-sampling steps match the full-step backward process as much as possible Kong and Ping [2021], Bao et al. [2021, 2022]. However, this would inevitably cause downgraded sample quality if each step is Gaussian: as discussed in Salimans and Ho [2021] and Xiao et al. [2021], a multi-step Gaussian sampler cannot be distilled into a one-step Gaussian sampler without loss of fidelity.

3.2 Problem Formulation

In both cases mentioned above, there might exist paths other than imitating the backward process that can reach the data distribution with fewer Gaussian steps. Thus one may expect to overcome these issues by minimizing the IPM.

Here we present the formulation of our problem setting. We assume that there is a target data distribution q_0 . Given a set of critic parameters \mathcal{A} s.t. $\Phi(p_0^{\theta},q_0)=\sup_{\alpha\in\mathcal{A}}g(p_0^{\theta},f_{\alpha},q_0)$ is an IPM, and given a DDPM sampler with T steps parameterized by θ , our goal is to solve:

$$\min_{\theta} \Phi(p_0^{\theta}, q_0). \tag{10}$$

3.3 Pathwise Derivative Estimation for Shortcut Fine-Tuning: Properties and Potential Issues

One straightforward approach is to optimize $\Phi(p_0^\theta,q_0)$ using pathwise derivative estimation [Rezende et al., 2014] like GAN training, which we denote as **SFT** (shortcut fine-tuning). We can recursively define the stochastic mappings:

$$h_{\theta,T}(x_T) := x_T,\tag{11}$$

$$h_{\theta,t}(x_t) := \mu_{\theta}(h_{\theta,t+1}(x_{t+1})) + \epsilon_{t+1},$$
 (12)

$$x_0 = h_{\theta,0}(x_T) \tag{13}$$

where $x_T \sim \mathcal{N}(0, I), \epsilon_{t+1} \sim \mathcal{N}(0, \Sigma_{t+1}), t = 0, ..., T - 1.$

Then we can write the objective function as:

$$\Phi(p_0^{\theta}, q_0) = \sup_{\alpha \in \mathcal{A}} \mathbb{E}_{x_T, \epsilon_{1:T}} [f_{\alpha}(h_{\theta, 0}(x_T))] - \mathbb{E}_{x_0 \sim q_0} [f_{\alpha}(x_0)]$$

$$\tag{14}$$

Assume that $\exists \alpha \in \mathcal{A}$, s.t. $g(p_0^{\theta}, \alpha, q_0) = \Phi(p_0^{\theta}, q_0)$. Let $\alpha^*(p_0^{\theta}, q_0) \in \{\alpha : g(p_0^{\theta}, \alpha, q_0) = \Phi(p_0^{\theta}, q_0)\}$. When f_{α} is 1-Lipschitz, we can compute the gradient which is similar to WGAN [Arjovsky et al., 2017]:

$$\nabla_{\theta} \Phi(p_0^{\theta}, q_0) = \mathbb{E}_{x_T, \epsilon_{1, T}} \left[\nabla_{\theta} f_{\alpha * (p_0^{\theta}, q_0)}(h_{\theta, 0}(x_T)) \right]. \tag{15}$$

Requirements on the family of critics \mathcal{A} . In Eq. (15), we can observe that the critic $f_{\alpha}*$ needs to provide meaningful gradients (w.r.t. the input) for the generator. If the gradient of the critic happens to be 0 at some generated data points, even if the critic's value could still make sense, the critic would provide no signal for the generator on these points⁴. Thus GANs trained with IPMs generally need to choose \mathcal{A} such that the gradient of the critic is regularized: For example, Lipschitz constraints like weight clipping [Arjovsky et al., 2017] and gradient penalty [Gulrajani et al., 2017] have been used for WGAN, and relatively wide kernel widths are used in MMD GAN [Li et al., 2017].

Potential issues. There might be some issues when computing Eq. (15) in practice. It contains differentiating a composite function with T steps, which faces similar problems when training RNNs:

- Gradient vanishing may result in long-distance dependency being lost;
- Gradient explosion may occur;
- Memory usage is high.

⁴For example, MMD with very narrow kernels can produce such critic functions, where each data point defines the center of the corresponding kernel which yields gradient 0.

4 Method: Shortcut Fine-Tuning with Policy Gradient (SFT-PG)

We note that Eq. (15) is not the only way to estimate the gradient w.r.t. IPM. In this section, we show that performing gradient descent of $\Phi(p_0^{\theta}, q_0)$ can be equivalent to policy gradient (Section 4.1), provide analysis towards monotonic improvement (Section 4.2) and algorithm design (Section 4.3).

4.1 Policy Gradient Equivalence

By modeling the conditional probability through the trajectory, we provide an alternative way for gradient estimation which is equivalent to policy gradient, without differentiating through the composite functions.

Theorem 4.1. (Policy gradient equivalence)

Assume that both $p_{x_{0:T}}^{\theta}(x_{0:T})f_{\alpha*(p_0^{\theta},q_0)}(x_0)$ and $\nabla_{\theta}p_{x_{0:T}}^{\theta}(x_{0:T})f_{\alpha*(p_0^{\theta},q_0)}(x_0)$ are continuous functions w.r.t. θ and $x_{0:T}$. Then

$$\nabla_{\theta} \Phi(p_0^{\theta}, q_0) = \mathbb{E}_{p_{x_0; T}^{\theta}} \left[f_{\alpha * (p_0^{\theta}, q_0)}(x_0) \nabla_{\theta} \log \sum_{t=0}^{T-1} p_t^{\theta}(x_t | x_{t+1}) \right].$$
 (16)

Proof.

$$\nabla_{\theta} \Phi(p_0^{\theta}, q_0) = \nabla_{\theta} \int p_0^{\theta}(x_0) f_{\alpha * (p_0^{\theta}, q_0)}(x_0) dx_0 + \nabla_{\theta} \alpha^*(p_0^{\theta}, q_0) \nabla_{\alpha * (p_0^{\theta}, q_0)} \int p_0^{\theta}(x_0) f_{\alpha * (p_0^{\theta}, q_0)}(x_0) dx_0,$$
(17)

where $\nabla_{\alpha*(p_0^{\theta},q_0)} \int p_0^{\theta}(x_0) f_{\alpha*(p_0^{\theta},q_0)}(x_0) dx_0$ is 0 from the envelope theorem. Then we have

$$\nabla_{\theta} \int p_{0}^{\theta}(x_{0}) f_{\alpha * (p_{0}^{\theta}, q_{0})}(x_{0}) dx_{0}$$

$$= \nabla_{\theta} \int \left(\int p_{x_{0:T}}^{\theta}(x_{0:T}) dx_{1:T} \right) f_{\alpha * (p_{0}^{\theta}, q_{0})}(x_{0}) dx_{0},$$

$$= \nabla_{\theta} \int p_{x_{0:T}}^{\theta}(x_{0:T}) f_{\alpha * (p_{0}^{\theta}, q_{0})}(x_{0}) dx_{0:T}$$

$$= \int p_{x_{0:T}}^{\theta}(x_{0:T}) f_{\alpha * (p_{0}^{\theta}, q_{0})}(x_{0}) \nabla_{\theta} \log p_{x_{0:T}}^{\theta}(x_{0:T}) dx_{0:T}$$

$$= \underset{p_{x_{0:T}}^{\theta}}{\mathbb{E}} \left[f_{\alpha * (p_{0}^{\theta}, q_{0})}(x_{0}) \sum_{t=0}^{T-1} \nabla_{\theta} \log p_{t}^{\theta}(x_{t}|x_{t+1}) \right],$$
(18)

where the second last equality is from the continuous assumptions to exchange integral and derivative and the \log derivative trick.

MDP construction for policy gradient equivalence. Here we explain why Eq. (16) could be viewed as policy gradient. We can construct an MDP with a finite horizon T: Treat $p_t^{\theta}(x_t|x_{t+1})$ as a policy, and assume that transition is an identical mapping such that the action is to choose the next state. Consider reward as $f_{\alpha*(p_0^{\theta},q_0)}(x_0)$ at the final step, and as 0 at any other steps. Then Eq. (16) is equivalent to performing policy gradient [Williams, 1992].

Comparing Eq. (15) and Eq. (16):

- Eq. (15) uses the gradient of the critic, while Eq. (16) only uses the value of the critic. This indicates that for policy gradient, weaker conditions are required for critics to provide meaningful guidance for the generator, which means more choices of \mathcal{A} can be applied here.
- We compute the sum of gradients for each step in Eq. (16), which does not suffer from exploding or vanishing gradients. Also, we do not need to track gradients of the generated sequence during T steps.
- However, policy gradient methods usually suffer from higher variance [Mohamed et al., 2020]. Thanks to similar techniques in RL, we can reduce the variance via a baseline trick, which will be discussed in Section 4.3.1.

In conclusion, Eq. (16) is comparable to Eq. (15) in expectation, with benefits such as numerical stability, memory efficiency, and more choices of \mathcal{A} . It could suffer from higher variance but the baseline trick can help. We denote such kind of method as **SFT-PG** (shortcut fine-tuning with policy gradient).

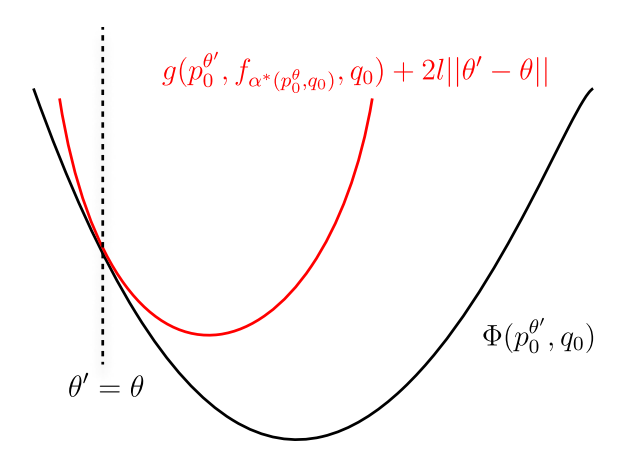


Figure 2: Illustration of the surrogate function given a fixed critic (red), and the actual objective $\Phi(p_0^{\theta'}, q_0)$ (dark). The horizontal axis represents the variable θ' . Starting from θ , a descent in the surrogate function is a sufficient condition for a descent in $\Phi(p_0^{\theta'}, q_0)$.

Empirical comparison. We also conduct experiments on some toy datasets (Fig 3), where we show the performance of Eq. (16) with the baseline trick is at least comparable to Eq. (15) at convergence when they use the same gradient penalty (GP) for critic regularization. We further observe SFT-PG with a new baseline regularization (B) has a noticeably better final performance compared to SFT with gradient penalty. The regularization methods will be introduced in Section 4.3.2. Details are in Section 6.2.2.

4.2 Towards Monotonic Improvement

The gradient update discussed in Eq. (15) or Eq. (16) only supports one step of gradient update, given a fixed critic $f_{\alpha*(p_0^\theta,q_0)}$ that is optimal to the current θ . Some questions remain: When is our update guaranteed to get improvement? Can we do more than one gradient step to get a potential descent? We answer the questions by providing a surrogate function of the IPM.

Theorem 4.2. (The surrogate function of IPM)

Assume that $g(p_0^{\theta}, f_{\alpha}, q_0)$ is Lipschitz w.r.t. θ , given q_0 and $\alpha \in A$. Given a fixed critic $f_{\alpha*(p_0^{\theta}, q_0)}$, there exists $l \ge 0$ such that $\Phi(p_0^{\theta'}, q_0)$ is upper bounded by the surrogate function below:

$$\Phi(p_0^{\theta'}, q_0) \leq g(p_0^{\theta'}, f_{\alpha * (p_0^{\theta}, q_0)}, q_0) + 2l||\theta' - \theta||.$$
(19)

Proof of Theorem 4.2 can be found in Appendix B. Here we provide an illustration of Theorem 4.2 in Fig 2. Given a critic that is optimal w.r.t. θ , $\Phi(p_0^{\theta'}, q_0)$ is unknown if $\theta \neq \theta'$. But if we can get a descent of the surrogate function, we are also guaranteed to get a descent of $\Phi(p_0^{\theta'}, q_0)$, which facilitates more potential updates even if $\theta' \neq \theta$.

Moreover, using the Lagrange multiplier, we can convert minimizing the surrogate function to a constrained optimization problem to optimize $g(p_0^{\theta'}, f_{\alpha^*(p_0^{\theta}, q_0)}, q_0)$ with the constraint that $||\theta' - \theta|| \le \delta$ for some $\delta > 0$. Following this idea, one simple trick is to perform $n_{\text{generator}}$ steps of gradient updates with a small learning rate, and clip the gradient norm with threshold γ . We present the empirical effect of such simple modification in Section 6.2.3, Table 2.

Discussion. One may notice that Theorem 4.2 is similar in spirit to Theorem 1 in TRPO [Schulman et al., 2015a], which provides a surrogate function for a fixed but unknown reward function. In our case, the reward function $f_{\alpha*(p_0^{\theta},q_0)}$ is known for the current θ but changing: It is dependent on the current θ so it remains unknown for $\theta' \neq \theta$. The proof techniques are also different, but they both estimate an unknown part of the objective function.

4.3 Algorithm Design

In the previous sections, we only consider the case where we have an optimal critic function given θ . In the training, we adopt similar techniques in WGAN [Arjovsky et al., 2017] to perform alternative training of the critic and generator in

order to approximate the optimal critic. Consider the objective function below:

$$\min_{\theta} \max_{\alpha \in \mathcal{A}} g(p_0^{\theta}, f_{\alpha}, q_0). \tag{20}$$

Now we discuss techniques to reduce the variance of the gradient estimation and regularize the critic, and then give an overview of our algorithm.

4.3.1 Baseline Function for Variance Reduction

Given a critic α , we can adopt a technique widely used in RL to reduce the variance of the gradient estimation in Eq. (16). Similar to Schulman et al. [2015b], we can subtract a baseline function $V_{t+1}^{\omega}(x_{t+1})$ from the cumulative reward $f_{\alpha}(x_0)$, without changing the expectation:

$$\nabla_{\theta} g(p_{0}^{\theta}, f_{\alpha}, q_{0})$$

$$= \underset{p_{x_{0:T}}^{\theta}}{\mathbb{E}} \left[f_{\alpha}(x_{0}) \sum_{t=0}^{T-1} \nabla_{\theta} \log p_{t}^{\theta}(x_{t}|x_{t+1}) \right]$$

$$= \underset{p_{x_{0:T}}^{\theta}}{\mathbb{E}} \left[\sum_{t=0}^{T-1} (f_{\alpha}(x_{0}) - V_{t+1}^{\omega}(x_{t+1})) \nabla_{\theta} \log p_{t}^{\theta}(x_{t}|x_{t+1}) \right],$$
(21)

where the optimal choice of $V_{t+1}^{\omega}(x_{t+1})$ to minimize the variance would be $V_{t+1}(x_{t+1},\alpha) := \underset{p_{x_{0:T}}^{\theta}}{\mathbb{E}} \left[f_{\alpha}(x_0) | x_{t+1} \right]$.

Detailed derivation of Eq (21) can be found in Appendix C. Thus, given a critic α and a generator θ , we can train a value function V_{t+1}^{ω} by minimizing the objective below:

$$R_B(\alpha, \omega, \theta) = \mathbb{E}_{p_{x_{0:T}}^{\theta}} \left[\sum_{t=0}^{T-1} (V_{t+1}^{\omega}(x_{t+1}) - V_{t+1}(x_{t+1}, \alpha))^2 \right].$$
 (22)

4.3.2 Choices of A: Regularizing the Critic

Here we discuss different choices of A, which indicates different regularization methods for the critic.

Lipschitz regularization. If we choose A to include parameters of all 1-Lipschitz functions, we can adopt regularization as WGAN-GP [Gulrajani et al., 2017]:

$$R_{GP}(\alpha, \theta) = \underset{\vec{x_0}}{\mathbb{E}} \left[\left(\left| \left| \nabla_{x_0} f_{\alpha}(x_0) \right| \right| - 1 \right)^2 \right], \tag{23}$$

where $\hat{x_0}$ is sampled uniformly on the line segment between $x_0' \sim p_0^{\theta}$ and $x_0'' \sim q_0$. f_{α} can be trained to maximize $g(p_0^{\theta}, f_{\alpha}, q_0) - \eta R_{GP}(\alpha, \omega, \theta), \eta > 0$ is the regularization coefficient.

Baseline as critic regularization. As discussed in Section 4.1, since we only use the critic value during updates, now we can consider a potentially wider range of choices for \mathcal{A} . Some regularization on f_{α} is still needed; Otherwise, its value can explode. Regularization is also shown to be beneficial for local convergence [Mescheder et al., 2018]. So we consider regularization that can be weaker than gradient constraints, such that the critic is more sensitive to the changes of the generator, which could be favorable when updating the critic for a fixed number of training steps.

We found an interesting fact that the loss $R_B(\alpha, \omega, \theta)$ can be *reused* to regularize the value of f_α , which implicitly defines a set \mathcal{A} that shows empirical benefits in practice.

Let

$$L(\alpha, \omega, \theta) = g(p_0^{\theta}, f_{\alpha}, q_0) - \lambda R_B(\alpha, \omega, \theta).$$
(24)

Given θ , our critic α and baseline ω can be trained together to maximize $L(\alpha, \omega, \theta)$.

We provide an explanation of such kind of implicit regularization. During the update, we can view V_{t+1}^{ω} as an approximation of the expected value of f_{α} from the previous step. The regularization provides a trade-off between maximizing $g(p_0^{\theta}, f_{\alpha}, q_0)$ and minimizing changes in the expected value of f_{α} , preventing drastic changes in the critic and stabilizing the training. Intuitively, it helps local convergence when both the critic and generator are already near-optimal: there is an extra cost for the critic value to diverge away from the optimal value. As a byproduct, it also makes the baseline function easier to fit.

Empirical comparison: baseline regularization and gradient penalty. We present a comparison of gradient penalty (GP) and baseline regularization (B) during policy gradient training (SFT-PG) in Section 6.2.2, Fig 3 on toy datasets, which shows in policy gradient training, the baseline function performs comparably well or better than gradient penalty.

4.3.3 Putting Together: Algorithm Overview

Now we are ready to present our algorithm. Our critic α and baseline ω is trained to maximize $L(\alpha, \omega, \theta)$, and the generator is trained to minimize $g(p_0^{\theta}, f_{\alpha}, q_0)$ via Eq. (21). These steps are performed alternatively. See details in Alg 1.

Algorithm 1 Shortcut Fine-Tuning with Policy Gradient and Baseline regularization: SFT-PG (B)

Input: n_{critic} , $n_{\text{generator}}$, batch size m, critic parameters α , baseline function parameter ω , pretrained generator $\overline{\theta}$, regularization hyperparameter λ

```
while \theta not converged do

Initialize trajectory buffer \mathcal{B} as \emptyset

for \mathbf{t} = 0,...,n_{\text{critic}} do

Obtain m i.i.d. samples from p_{x_0:T}^{\theta} and add to \mathcal{B}

Obtain m i.i.d. samples from q_0

Update \alpha and \omega via maximizing Eq. (24)

end for

for \mathbf{t} = 0,...,n_{\text{generator}} do

Obtain m samples according to p_{x_0:T}^{\theta} from \mathcal{B}

Update \theta via policy gradient according to Eq. (21)

end for

end while
```

5 Related Works

GAN and RL. There are works using ideas from RL to train GANs [Yu et al., 2017, Wang et al., 2017, Sarmad et al., 2019, Bai et al., 2019]. The most relevant work is SeqGAN [Yu et al., 2017], and our work differs in the following ways: The next token is dependent on all previous tokens in SeqGAN, which is not the case in diffusion models. The critic takes the whole sequence as input in SeqGAN, while we only care about the final state. Besides, in our work, rewards are derived from performing gradient descent w.r.t. IPM, while in SeqGAN, rewards are designed manually.

Diffusion and GAN. There are other works combining diffusion and GAN training: Xiao et al. [2021] consider a more complicated noise distribution generated by GAN to enable fast sampling; Diffusion GAN [Wang et al., 2022] perturbs the data with an adjustable number of steps, and minimizes JS divergence for each step using GAN training. To our best knowledge, there is no existing work using GAN training to directly fine-tune a pretrained DDPM sampler.

Deterministic fast samplers of DDIM. There is another line of work on fast sampling of DDIM [Song et al., 2020a], for example, knowledge distillation [Luhman and Luhman, 2021, Salimans and Ho, 2021] and solving ordinary differential equations (ODEs) [Watson et al., 2021b, Liu et al., 2022, Lu et al., 2022]. Fast sampling is easier for DDIM samplers (with deterministic Markov chains) than DDPM samplers (with conditional Gaussian Markov chains), since it is possible to combine multiple deterministic steps into one step without loss of fidelity, but not for stochastic steps, especially when combining multiple Gaussian steps into one Gaussian [Salimans and Ho, 2021]. There is also a contemporary work that fine-tunes a DDIM sampler using MMD calculated by a pretrained feature space and a cubic kernel [Aiello et al., 2023], which is similar to Section 3.3 but with a fixed critic and a deterministic sampler. Besides the potential issues discussed in Section 3.3, we also note that adversarially trained critics provide stronger signals when $p_0^\theta \neq q_0$ than fixed ones [Li et al., 2017]. As a result, the latter may yield sub-optimal results when p_0^θ is not close enough to q_0 at initialization, and is also highly dependent on the choice of the critic.

6 Experiments

In this section, we aim to answer the following questions:

• (Section 6.2.1) Does the proposed algorithm SFT-PG (B) work in practice?

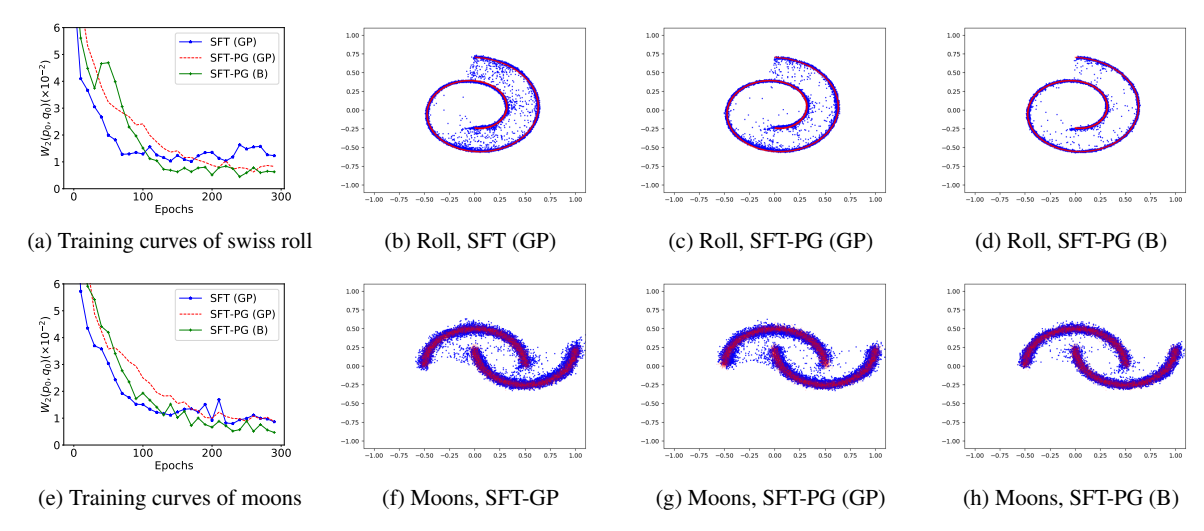


Figure 3: Training curves (3a, 3e) and 10K randomly generated samples from SFT (GP) (3b, 3f), SFT-PG (GP) (3c, 3g), and SFT-PG (B) (3d, 3h) at convergence. In the visualizations, red dots indicate the ground truth distribution, and blue dots indicate generated distribution. We can observe that SFT-PG (B) generates noticeably better distributions.

- (Section 6.2.2) How does SFT-PG (Eq. (16)) work compared to SFT (Eq. (15)) with the same regularization (GP), and how does baseline regularization (B) compared to gradient penalty (GP) in SFT-PG?
- (Section 6.2.3) Do more generator steps with gradient clipping improve the performance, as discussed in Section 4.2?
- (Section 6.3) Can the proposed objective improve existing fast samplers of DDPM on benchmark datasets?

Code is available at https://github.com/UW-Madison-Lee-Lab/SFT-PG.

6.1 Setup

Here we provide the setup of our training algorithm on different datasets. Model architectures and more training details can be found in Appendix D.

Toy datasets. The toy datasets we use are swiss roll and two moons [Pedregosa et al., 2011]. We use $\lambda = 0.1$, $n_{\text{critic}} = 5$, $n_{\text{generator}} = 1$ with no gradient clipping. For evaluation, we use the Wasserstein-2 distance on 10K samples from p_0 and q_0 respectively, calculated by POT [Flamary et al., 2021].

Image datasets. We use MNIST [LeCun et al., 1998], CIFAR-10 [Krizhevsky et al., 2009] and CelebA [Liu et al., 2015]. For hyperparameters, we choose $\lambda=1.0$, $n_{\text{critic}}=5$, $n_{\text{generator}}=5$, $\gamma=0.1$, except when testing different choices of $n_{\text{generator}}$ and γ . For evaluation, we use the FID [Heusel et al., 2017] measured by 50K samples generated from p_0^θ and q_0 respectively.

6.2 Proof-of-concept Results

In this section, we fine-tune pretrained DDPMs with T=10, and present the effect of the proposed algorithm on toy datasets, and show the results of different gradient estimations discussed in Section 4.1, different critic regularization methods discussed in Section 4.2, and the training technique with more steps discussed Section 4.2.

6.2.1 Improvement from Fine-Tuning

On the swiss roll dataset, we first train a DDPM with T=10 till convergence, and then use it as initialization of our fine-tuning. As in Table 1, our fine-tuned sampler with 10 steps can get better Wasserstein distance not only compared to the DDPM with T=10, but can even outperform DDPM with T=1000, which is reasonable since we directly optimize the IPM objective. ⁵ The training curve and the data visualization can be found in Fig 3a and Fig 3d.

⁵Besides, training from scratch using our algorithm also works, with a final performance comparable to fine-tuning.

Method	$\mathbf{W_2}(\mathbf{p_0^{\theta}}, \mathbf{q_0}) \times 10^{-2}) \left(\downarrow\right)$
T= 10, DDPM	8.29
T=100, DDPM	2.36
T= 1000, DDPM	1.78
T=10, SFT-PG (B)	0.64

Table 1: Comparison of DDPM models and our fine-tuned model on the swiss roll dataset.

6.2.2 Effect of Different Gradient Estimations and Regularizations

On the toy datasets, we compare gradient estimation SFT-PG and SFT, both with gradient penalty (GP). 6 We also compare them to our proposed algorithm SFT-PG (B). All methods are initialized with pretrained DDPM, T=10, then trained till convergence. As shown in Fig 3, we can observe that all methods converge and the training curves are almost comparable, while SFT-PG (B) enjoys a slightly better final performance.

6.2.3 Effect of Gradient Clipping with More Steps

In Section 4.2, we discussed that performing more generator steps with the same fixed critic and meanwhile clipping the gradient norm can improve the training of our algorithm. Here we present the effect of $n_{\rm generator}=1$ or 5 with different gradient clipping thresholds γ on MNIST, initialized with a pretrained DDPM with T=10, FID=7.34. From Table 2, we find that a small γ with more steps can improve the final performance, but could hurt the performance if too small. Randomly generated samples from the model with the best FID are in Fig 4. We also conducted similar experiments on the toy datasets, but we find no significant difference. We believe that this is because the task is too simple.

Method	$FID(\downarrow)$
1 step	1.35
5 steps, $\gamma = 10$	0.83
5 steps, $\gamma = 1.0$	0.82
5 steps, $\gamma = 0.1$	0.89
5 steps, $\gamma = 0.001$	1.46



Table 2: Effect of $n_{\text{generator}}$ and γ , trained on MNIST.

Figure 4: Randomly generated samples, trained on MNIST.

6.3 Benchmark Results

In this section, we take pretrained DDPMs with T = 1000 and fine-tune them with sampling steps T' = 10 to compare with existing fast samplers of DDPM on image benchmark datasets CIFAR-10 and CelebA.

Our baselines include various fast samplers of DDPM with Gaussian noises: naive DDPM sub-sampling, Fast-DPM [Kong and Ping, 2021], and recently advanced DDPM samplers like Analytic DPM [Bao et al., 2021] and SN-DPM [Bao et al., 2022]. For fine-tuning, we use the fixed variance and sub-sampling schedules computed by FastDPM with T'=10 and only train the mean prediction model. From Table 3, we can observe that the performance of fine-tuning with T'=10 is comparable to the pretrained model with T=1000, outperforming the existing DDPM samplers. Randomly generated images before and after fine-tuning are in Fig 5.

Method	CIFAR-10 (32×32)	CelebA (64 × 64)
DDPM	34.76	36.69
FastDPM	29.43	28.98
Analytic-DPM	22.94	28.99
SN-DDPM	16.33	20.60
SFT-PG (B)	2.59	3.34

Table 3: FID (\downarrow) on CIFAR-10 and CelebA, T'=10 for all methods. Our fine-tuning produces comparable results with the full-step pretrained models (T=1000, FID = 3.03 for CIFAR-10, and FID = 3.26 for CelebA).

⁶For gradient penalty coefficient, we tested different choices in [0.001, 10] and pick the best choice 0.001. We also tried spectral normalization for Lipschitz constraints, but we found that its performance is worse than gradient penalty on these datasets.

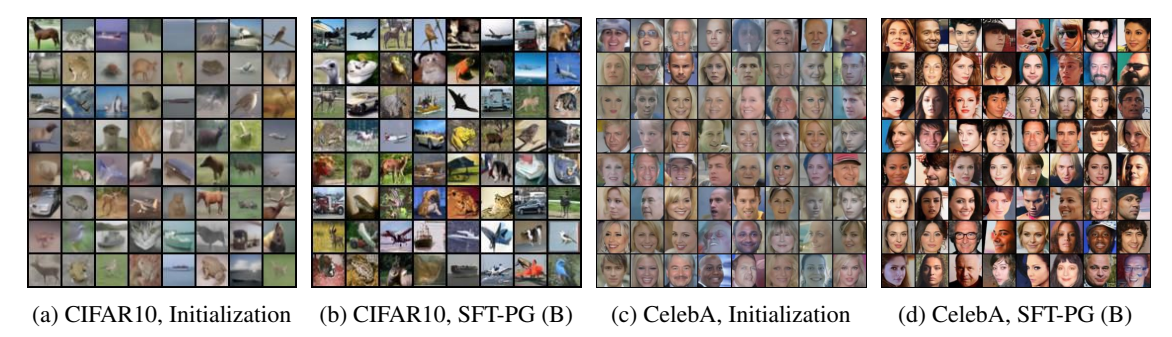


Figure 5: Randomly generated images before and after fine-tuning, on CIFAR10 (32×32) and CelebA (64×64) , T' = 10. The initialization is from pretrained models with T = 1000 and sub-sampling schedules with T' = 10 calculated from FastDPM [Kong and Ping, 2021].

6.4 Discussions and Limitations

In our experiments, we only train the mean prediction model given a pretrained DDPM. It is also possible to learn the variance via fine-tuning with the same objective, and we leave it as future work. We also note that although we do not need to track the gradients during all sampling steps, we still need to run T' inference steps to collect the sequence, which is inevitably slower than the 1-step GAN training.

7 Conclusion

In this work, we fine-tune DDPM samplers to minimize the IPMs via policy gradient. We show performing gradient descent of stochastic Markov chains w.r.t. IPM is equivalent to policy gradient, and present a surrogate function of the IPM which sheds light on monotonic improvement conditions. Our fine-tuning improves the existing fast samplers of DDPM, achieving comparable or even higher sample quality than the full-step model on various datasets.

References

Jonathan Ho, Ajay Jain, and Pieter Abbeel. Denoising diffusion probabilistic models. *Advances in Neural Information Processing Systems*, 33:6840–6851, 2020.

Alexander Quinn Nichol and Prafulla Dhariwal. Improved denoising diffusion probabilistic models. In *International Conference on Machine Learning*, pages 8162–8171. PMLR, 2021.

Prafulla Dhariwal and Alexander Nichol. Diffusion models beat gans on image synthesis. *Advances in Neural Information Processing Systems*, 34:8780–8794, 2021.

Ian Goodfellow, Jean Pouget-Abadie, Mehdi Mirza, Bing Xu, David Warde-Farley, Sherjil Ozair, Aaron Courville, and Yoshua Bengio. Generative adversarial nets. In Z. Ghahramani, M. Welling, C. Cortes, N. Lawrence, and K.Q. Weinberger, editors, *Advances in Neural Information Processing Systems*, volume 27, 2014.

Zhifeng Kong and Wei Ping. On fast sampling of diffusion probabilistic models. *arXiv preprint arXiv:2106.00132*, 2021.

Robin San-Roman, Eliya Nachmani, and Lior Wolf. Noise estimation for generative diffusion models. *arXiv preprint arXiv:2104.02600*, 2021.

Max WY Lam, Jun Wang, Rongjie Huang, Dan Su, and Dong Yu. Bilateral denoising diffusion models. *arXiv preprint* arXiv:2108.11514, 2021.

Daniel Watson, Jonathan Ho, Mohammad Norouzi, and William Chan. Learning to efficiently sample from diffusion probabilistic models. *arXiv preprint arXiv:2106.03802*, 2021a.

Alexia Jolicoeur-Martineau, Ke Li, Rémi Piché-Taillefer, Tal Kachman, and Ioannis Mitliagkas. Gotta go fast when generating data with score-based models. *arXiv preprint arXiv:2105.14080*, 2021.

Fan Bao, Chongxuan Li, Jun Zhu, and Bo Zhang. Analytic-dpm: an analytic estimate of the optimal reverse variance in diffusion probabilistic models. In *International Conference on Learning Representations*, 2021.

Fan Bao, Chongxuan Li, Jiacheng Sun, Jun Zhu, and Bo Zhang. Estimating the optimal covariance with imperfect mean in diffusion probabilistic models. In *International Conference on Machine Learning*, pages 1555–1584. PMLR, 2022.

- Eliya Nachmani, Robin San Roman, and Lior Wolf. Non gaussian denoising diffusion models. *arXiv preprint* arXiv:2106.07582, 2021.
- Zhisheng Xiao, Karsten Kreis, and Arash Vahdat. Tackling the generative learning trilemma with denoising diffusion gans. In *International Conference on Learning Representations*, 2021.
- Jiaming Song, Chenlin Meng, and Stefano Ermon. Denoising diffusion implicit models. In *International Conference on Learning Representations*, 2020a.
- Ahmed Hussein, Mohamed Medhat Gaber, Eyad Elyan, and Chrisina Jayne. Imitation learning: A survey of learning methods. *ACM Computing Surveys (CSUR)*, 50(2):1–35, 2017.
- Mel Vecerik, Todd Hester, Jonathan Scholz, Fumin Wang, Olivier Pietquin, Bilal Piot, Nicolas Heess, Thomas Rothörl, Thomas Lampe, and Martin Riedmiller. Leveraging demonstrations for deep reinforcement learning on robotics problems with sparse rewards. *arXiv* preprint arXiv:1707.08817, 2017.
- Yang Song, Jascha Sohl-Dickstein, Diederik P Kingma, Abhishek Kumar, Stefano Ermon, and Ben Poole. Score-based generative modeling through stochastic differential equations. In *International Conference on Learning Representations*, 2020b.
- Dohyun Kwon, Ying Fan, and Kangwook Lee. Score-based generative modeling secretly minimizes the wasserstein distance. In *Advances in Neural Information Processing Systems*, 2022.
- Tim Salimans and Jonathan Ho. Progressive distillation for fast sampling of diffusion models. In *International Conference on Learning Representations*, 2021.
- Danilo Jimenez Rezende, Shakir Mohamed, and Daan Wierstra. Stochastic backpropagation and approximate inference in deep generative models. In *International conference on machine learning*, pages 1278–1286. PMLR, 2014.
- Martin Arjovsky, Soumith Chintala, and Léon Bottou. Wasserstein generative adversarial networks. In *International conference on machine learning*, pages 214–223. PMLR, 2017.
- Ishaan Gulrajani, Faruk Ahmed, Martin Arjovsky, Vincent Dumoulin, and Aaron C Courville. Improved training of wasserstein gans. *Advances in neural information processing systems*, 30, 2017.
- Chun-Liang Li, Wei-Cheng Chang, Yu Cheng, Yiming Yang, and Barnabás Póczos. Mmd gan: Towards deeper understanding of moment matching network. *Advances in neural information processing systems*, 30, 2017.
- Ronald J Williams. Simple statistical gradient-following algorithms for connectionist reinforcement learning. *Reinforcement learning*, pages 5–32, 1992.
- Shakir Mohamed, Mihaela Rosca, Michael Figurnov, and Andriy Mnih. Monte carlo gradient estimation in machine learning. *J. Mach. Learn. Res.*, 21(132):1–62, 2020.
- John Schulman, Sergey Levine, Pieter Abbeel, Michael Jordan, and Philipp Moritz. Trust region policy optimization. In *International conference on machine learning*, pages 1889–1897. PMLR, 2015a.
- John Schulman, Philipp Moritz, Sergey Levine, Michael Jordan, and Pieter Abbeel. High-dimensional continuous control using generalized advantage estimation. *arXiv preprint arXiv:1506.02438*, 2015b.
- Lars Mescheder, Andreas Geiger, and Sebastian Nowozin. Which training methods for gans do actually converge? In *International conference on machine learning*, pages 3481–3490. PMLR, 2018.
- Lantao Yu, Weinan Zhang, Jun Wang, and Yong Yu. Seqgan: Sequence generative adversarial nets with policy gradient. In *Proceedings of the AAAI conference on artificial intelligence*, volume 31, 2017.
- Jun Wang, Lantao Yu, Weinan Zhang, Yu Gong, Yinghui Xu, Benyou Wang, Peng Zhang, and Dell Zhang. Irgan: A minimax game for unifying generative and discriminative information retrieval models. In *Proceedings of the 40th International ACM SIGIR conference on Research and Development in Information Retrieval*, pages 515–524, 2017.
- Muhammad Sarmad, Hyunjoo Jenny Lee, and Young Min Kim. Rl-gan-net: A reinforcement learning agent controlled gan network for real-time point cloud shape completion. In *Proceedings of the IEEE/CVF Conference on Computer Vision and Pattern Recognition*, pages 5898–5907, 2019.
- Xueying Bai, Jian Guan, and Hongning Wang. A model-based reinforcement learning with adversarial training for online recommendation. *Advances in Neural Information Processing Systems*, 32, 2019.
- Zhendong Wang, Huangjie Zheng, Pengcheng He, Weizhu Chen, and Mingyuan Zhou. Diffusion-gan: Training gans with diffusion. *arXiv preprint arXiv:2206.02262*, 2022.
- Eric Luhman and Troy Luhman. Knowledge distillation in iterative generative models for improved sampling speed. *arXiv preprint arXiv:2101.02388*, 2021.

- Daniel Watson, William Chan, Jonathan Ho, and Mohammad Norouzi. Learning fast samplers for diffusion models by differentiating through sample quality. In *International Conference on Learning Representations*, 2021b.
- Luping Liu, Yi Ren, Zhijie Lin, and Zhou Zhao. Pseudo numerical methods for diffusion models on manifolds. *arXiv* preprint arXiv:2202.09778, 2022.
- Cheng Lu, Yuhao Zhou, Fan Bao, Jianfei Chen, Chongxuan Li, and Jun Zhu. Dpm-solver: A fast ode solver for diffusion probabilistic model sampling in around 10 steps. *arXiv preprint arXiv:2206.00927*, 2022.
- Emanuele Aiello, Diego Valsesia, and Enrico Magli. Fast inference in denoising diffusion models via mmd finetuning. *arXiv preprint arXiv:2301.07969*, 2023.
- F. Pedregosa, G. Varoquaux, A. Gramfort, V. Michel, B. Thirion, O. Grisel, M. Blondel, P. Prettenhofer, R. Weiss, V. Dubourg, J. Vanderplas, A. Passos, D. Cournapeau, M. Brucher, M. Perrot, and E. Duchesnay. Scikit-learn: Machine learning in Python. *Journal of Machine Learning Research*, 12:2825–2830, 2011.
- Rémi Flamary, Nicolas Courty, Alexandre Gramfort, Mokhtar Z. Alaya, Aurélie Boisbunon, Stanislas Chambon, Laetitia Chapel, Adrien Corenflos, Kilian Fatras, Nemo Fournier, Léo Gautheron, Nathalie T.H. Gayraud, Hicham Janati, Alain Rakotomamonjy, Ievgen Redko, Antoine Rolet, Antony Schutz, Vivien Seguy, Danica J. Sutherland, Romain Tavenard, Alexander Tong, and Titouan Vayer. Pot: Python optimal transport. *Journal of Machine Learning Research*, 22(78):1–8, 2021.
- Yann LeCun, Léon Bottou, Yoshua Bengio, and Patrick Haffner. Gradient-based learning applied to document recognition. *Proceedings of the IEEE*, 86(11):2278–2324, 1998.
- Alex Krizhevsky, Geoffrey Hinton, et al. Learning multiple layers of features from tiny images. 2009.
- Ziwei Liu, Ping Luo, Xiaogang Wang, and Xiaoou Tang. Deep learning face attributes in the wild. In *Proceedings of the IEEE international conference on computer vision*, pages 3730–3738, 2015.
- Martin Heusel, Hubert Ramsauer, Thomas Unterthiner, Bernhard Nessler, and Sepp Hochreiter. Gans trained by a two time-scale update rule converge to a local nash equilibrium. *Advances in neural information processing systems*, 30, 2017.
- Diederik P Kingma and Jimmy Ba. Adam: A method for stochastic optimization. arXiv preprint arXiv:1412.6980, 2014.

A Illustration of the Issues when Sampling with $T' \ll T$ in DDPM

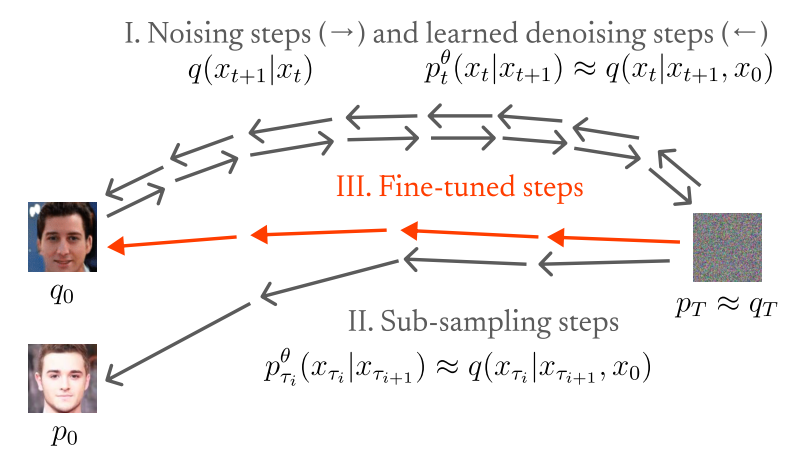


Figure 6: When T is large but we want a fast sampler, sub-sampling with $T' \ll T$ cannot approximate the backward process accurately when each step is Gaussian as discussed in Case 2, Section 3.1.

B Towards Monotonic Improvement

Here we present detailed proof of Theorem 4.2. For simplicity, we denote p_0^{θ} as p_{θ} , q_0 as q, and $z \in \mathbb{R}^d$ to replace x_0 as a variable in our sample space.

Recall the generated distribution: p_{θ} . Given target distribution q, the objective function is:

$$\min_{\theta} \max_{\alpha \in \mathcal{A}} g(p_{\theta}, f_{\alpha}, q), \tag{25}$$

where $g(p_{\theta}, f_{\alpha}, q) = \int (p_{\theta}(z) - q(z)) f_{\alpha}(z) dz$.

Recall
$$\Phi(p_{\theta}, q) = \max_{\alpha \in \mathcal{A}} \int (p_{\theta}(z) - q(z)) f_{\alpha}(z) dz = \int (p_{\theta}(z) - q(z)) f_{\alpha * (p_{\theta}, q)}(z) dz$$
.

Our goal is to show that there exists $l \ge 0$ s.t.:

$$\Phi(p_{\theta'}, q) \leq g(p_{\theta'}, f_{\alpha * (p_{\theta}, q)}, q) + 2l||\theta - \theta'||, \tag{26}$$

where the equality is achieved when $\theta = \theta'$.

If the above inequality holds, $L_{\theta}(\theta') = g(p_{\theta'}, f_{\alpha*(p_{\theta},q)}, q) + 2l||\theta - \theta'||$ can be a surrogate function of $\Phi(p_{\theta'}, q)$: $\Phi(p_{\theta'}, q) - \Phi(p_{\theta}, q) \leqslant L_{\theta}(\theta') - L_{\theta}(\theta)$, $L_{\theta}(\theta) = \Phi(p_{\theta}, q)$, which means θ' that can improve $L_{\theta}(\theta')$ is also guaranteed to get improvement on $\Phi(p_{\theta'}, q)$.

Proof. Consider

$$\Phi(p_{\theta'}, q) - \Phi(p_{\theta}, q)
= \int (p_{\theta'}(z) - q(z)) f_{\alpha *(p_{\theta'}, q)}(z) dz - \int (p_{\theta}(z) - q(z)) f_{\alpha *(p_{\theta}, q)}(z) dz
= \int (p_{\theta'}(z) - q(z)) f_{\alpha *(p_{\theta'}, q)}(z) dz - \int (p_{\theta'}(z) - q(z)) f_{\alpha *(p_{\theta}, q)}(z) dz
+ \int (p_{\theta'}(z) - q(z)) f_{\alpha *(p_{\theta}, q)}(z) dz - \int (p_{\theta}(z) - q(z)) f_{\alpha *(p_{\theta}, q)}(z) dz
= \int (p_{\theta'}(z) - q(z)) (f_{\alpha *(p_{\theta'}, q)}(z) - f_{\alpha *(p_{\theta}, q)}(z)) dz + \int (p_{\theta'}(z) - p_{\theta}(z)) f_{\alpha *(p_{\theta}, q)}(z) dz
= \int (q(z) - p_{\theta'}(z)) (f_{\alpha *(p_{\theta}, q)}(z) - f_{\alpha *(p_{\theta'}, q)}(z)) dz + \int (p_{\theta'}(z) - p_{\theta}(z)) f_{\alpha *(p_{\theta}, q)}(z) dz.$$
(27)

We have

$$\int (q(z) - p_{\theta'}(z))(f_{\alpha * (p_{\theta}, q)}(z) - f_{\alpha * (p_{\theta'}, q)}(z))dz
= \int (p_{\theta}(z) - p_{\theta'}(z))(f_{\alpha * (p_{\theta}, q)}(z) - f_{\alpha * (p_{\theta'}, q)}(z))dz - \int (p_{\theta}(z) - q(z))(f_{\alpha * (p_{\theta}, q)}(z) - f_{\alpha * (p_{\theta'}, q)}(z))dz
\leq \int (p_{\theta}(z) - p_{\theta'}(z))(f_{\alpha * (p_{\theta}, q)}(z) - f_{\alpha * (p_{\theta'}, q)}(z))dz,$$
(28)

where the last inequality comes from the definition $\alpha^*(p_\theta, q) = \underset{\alpha \in \mathcal{A}}{\arg \max} \int (p_\theta(z) - q(z)) f_\alpha(z)$.

So

$$\Phi(p_{\theta'}, q) - \Phi(p_{\theta}, q) = \int (p_{\theta'}(z) - p_{\theta}(z)) f_{\alpha * (p_{\theta}, q)}(z) dz + \int (q(z) - p_{\theta'}(z)) (f_{\alpha * (p_{\theta}, q)}(z) - f_{\alpha * (p_{\theta'}, q)}(z)) dz$$

$$\leq g(p_{\theta'}, f_{\alpha * (p_{\theta}, q)}, q) - g(p_{\theta}, f_{\alpha * (p_{\theta}, q)}, q) + \int (p_{\theta}(z) - p_{\theta'}(z)) (f_{\alpha * (p_{\theta}, q)}(z) - f_{\alpha * (p_{\theta'}, q)}(z)) dz$$

$$\leq g(p_{\theta'}, f_{\alpha * (p_{\theta}, q)}, q) - g(p_{\theta}, f_{\alpha * (p_{\theta}, q)}, q) + 2l||\theta - \theta'||, \tag{29}$$

where the last inequality comes from the Lipschitz assumption of $g(p_{\theta}, f_{\alpha(p_{\theta},q)}, q)$. Recall that $\Phi(p_{\theta}, q) = g(p_{\theta}, f_{\alpha*(p_{\theta},q)}, q)$, the proof is then complete.

Consider the optimization objective: minimize_{θ'} $L_{\theta}(\theta')$. Using the Lagrange multiplier, we can convert the problem to a constrained optimization problem:

where $\delta > 0$. The constraint is a convex set and the projection to the set is easy to compute via norm regularization, as we discussed in Section 4.2. Intuitively, it means that as long as we only optimize in the neighborhood of the current generator θ' , we can treat $g(p'_{\theta}, f_{\alpha*(p_{\theta},q)}, q)$ as a good approximation of $\Phi(p_{\theta'}, q)$ and use it as surrogation.

C Baseline Function for Variance Reduction

Here we present the derivation of Eq (21), which is very similar to Schulman et al. [2015b].

To show

$$\mathbb{E}_{p_{x_{0:T}}^{\theta}} \left[f_{\alpha}(x_{0}) \sum_{t=0}^{T-1} \nabla_{\theta} \log p_{t}^{\theta}(x_{t}|x_{t+1}) \right] = \mathbb{E}_{p_{x_{0:T}}^{\theta}} \left[\sum_{t=0}^{T-1} (f_{\alpha}(x_{0}) - V_{t+1}^{\omega}(x_{t+1})) \nabla_{\theta} \log p_{t}^{\theta}(x_{t}|x_{t+1}) \right], \quad (31)$$

we only need to show

$$\mathbb{E}_{p_{x_{0:T}}^{\theta}} \left[V_{t+1}^{\omega}(x_{t+1}) \nabla_{\theta} \log p_{t}^{\theta}(x_{t}|x_{t+1}) \right] = 0.$$
(32)

Note that

$$\mathbb{E}_{p_{x_{0:T}}^{\theta}} \left[V_{t+1}^{\omega}(x_{t+1}) \nabla_{\theta} \log p_{t}^{\theta}(x_{t}|x_{t+1}) \right]
= \mathbb{E}_{p_{x_{t+1:T}}^{\theta}} \left[\mathbb{E}_{p_{x_{0:t}}^{\theta}} \left[V_{t+1}^{\omega}(x_{t+1}) \nabla_{\theta} \log p_{t}^{\theta}(x_{t}|x_{t+1}) | x_{t+1:T} \right] \right]
= \mathbb{E}_{p_{x_{t+1:T}}^{\theta}} \left[\mathbb{E}_{p_{x_{t}}^{\theta}} \left[V_{t+1}^{\omega}(x_{t+1}) \nabla_{\theta} \log p_{t}^{\theta}(x_{t}|x_{t+1}) | x_{t+1:T} \right] \right],$$
(33)

where $\underset{p_{x_t}^{\theta}}{\mathbb{E}}\left[V_{t+1}^{\omega}(x_{t+1})\nabla_{\theta}\log p_t^{\theta}(x_t|x_{t+1})|x_{t+1:T}\right]=0$ when $p_t^{\theta}(x_t|x_{t+1})$ and $\nabla_{\theta}p_t^{\theta}(x_t|x_{t+1})$ are continuous:

$$\mathbb{E}_{p_{x_{t}}^{\omega}} \left[V_{t+1}^{\omega}(x_{t+1}) \nabla_{\theta} \log p_{t}^{\theta}(x_{t}|x_{t+1}) | x_{t+1:T} \right] \\
= V_{t+1}^{\omega}(x_{t+1}) \int p_{x_{t}}^{\theta}(x_{t}) \nabla_{\theta} \log p_{t}^{\theta}(x_{t}|x_{t+1}) dx_{t} \\
= V_{t+1}^{\omega}(x_{t+1}) \int p_{x_{t}}^{\theta}(x_{t}) \nabla_{\theta} \log p_{t}^{\theta}(x_{t}|x_{t+1}) dx_{t} \\
= V_{t+1}^{\omega}(x_{t+1}) \int \nabla_{\theta} p_{t}^{\theta}(x_{t}|x_{t+1}) dx_{t} \\
= V_{t+1}^{\omega}(x_{t+1}) \nabla_{\theta} \int p_{t}^{\theta}(x_{t}|x_{t+1}) dx_{t} \\
= V_{t+1}^{\omega}(x_{t+1}) \nabla_{\theta} \int p_{t}^{\theta}(x_{t}|x_{t+1}) dx_{t} \\
= 0. \tag{34}$$

D Experimental Details

Here we provide more details for our fine-tuning settings for reproducibility. We also provide the code base in the supplementary files.

D.1 Experiments on Toy Datasets

Training sets. For 2D toy datasets, each training set contains 10K samples.

Model architecture. The generator we adopt is a 4-layer MLP with 128 hidden units and soft-plus activations. The critic and the baseline function we use are 3-layer MLPs with 128 hidden units and ReLU activations.

Training details. For the optimizers, we use Adam [Kingma and Ba, 2014] with $lr = 5 \times 10^{-5}$ for the generator, and $lr = 1 \times 10^{-3}$ for both the critic and baseline functions. Pretraining for DDPM is conducted for 2000 epochs for T = 10, 100, 1000 repectively. Both pretraining and fine-tuning use batch size 64.

D.2 Experiments on Image Datasets

Training sets. We use 60K training samples from MNIST, 50K training samples from CIFAR-10, and 162K samples from CelebA.

Model architecture. We use U-Net architecture for image generation tasks as Ho et al. [2020]. For the critic, we adopt 3 convolutional layers with kernel size = 4, stride = 2, padding = 1 for downsampling, followed by 1 final convolutional layer with kernel size = 4, stride = 1, padding = 0, and then take the average of the final image. The numbers of output channels are 256,512,1024,1 for each layer, with Leaky ReLU (slope = 0.2) as activation. For the baseline function, we use a 4-layer MLP with time embeddings. The numbers of hidden units are 1024, 1024, 256, and the output size is 1.

Training details. For MNIST, we train a DDPM with T=10 steps for 100 epochs to convergence as a pretrained model. For CIFAR-10 and CelebA, we use the pretrained model in Ho et al. [2020] and Song et al. [2020a] with T=1000, and use the sampling schedules calculated by Fast-DPM [Kong and Ping, 2021] with VAR approximation as initialization for our fine-tuning. We found that rescaling the pixel values to [0,1] is a default choice in Fast-DPM, but it can hurt training if we feed rescaled images directly into the critic, so we remove the rescaling part in our fine-tuning. For the optimizers, we use Adam with $Ir=1\times10^{-6}$ for the generator, and $Ir=1\times10^{-4}$ for both the critic and baseline functions. For MNIST (60K training samples) and CIFAR-10 (50K training samples), we trained 100 epochs with batch size = 128. For CelebA (162K training samples) we trained 50 epochs with batch size = 64. We run these experiments on 4 RTX 2080Ti GPUs. It takes about 5h for CIFAR-10 and MNIST and about 24h for CelebA.